Enhanced Fast Frequency Response Strategy for Power Systems with Volatile Inertia

Kush Lohana, *el22kl@leeds.ac.uk*, Dr. Sadegh Azizi (Supervisor), and Dr. Paolo Actis (Assessor)

***Abstract*—The integration of renewables into power systems results in low inertia, leading to pronounced stability challenges. For contingency events, these low-inertia systems experience an accelerated rate of change of frequency (RoCoF) and deeper nadir frequencies, necessitating effective fast frequency response (FFR) mechanisms. While existing FFR research is grounded in the presumption that the shape of the injected power mirrors the generation loss, there remains an evident gap: the optimal shape of power injection to maximize system stability remains unexplored. The study introduces a novel approach to power system stability by exploring the concept of short-lived transient energy injection. It assesses the impact of this injection both independently and with conventional steady power injection. Additionally, the study identifies the boundary value conditions when transient energy is injected independently and evaluates its effectiveness and resilience during periods of volatile inertia and in situations with imprecise contingency size information. The findings, validated through implementation in PowerFactory, pave the way for further research into optimizing short-lived energy injections, which hold the potential to enhance post-contingency power system recovery and fortify frequency stability.**

***Index Terms*—Fast frequency response (FFR), Optimal power injection, Short-lived transient energy injection, Low-inertia system.**

I. Introduction

Balancing electricity generation and consumption is crucial for a stable power grid. Traditional grids adjust the supply based on demand predictions and real-time monitoring. However, as the world leans towards renewable energy sources (RES), modern grids focus on demand flexibility to compensate for the variable output of RES.

Frequency deviations in an AC grid, often triggered by significant imbalances like loss of generation or transmission lines, can have severe implications. Generators operate at a standard frequency of either 50 or 60 Hz and can only tolerate deviations within a narrow range. For instance, the UK grid mandates operation between 47.5 - 51.5 Hz range [1]; any deviation beyond this range may trip generators and lead to power blackouts.

A. Grid Inertia and Frequency Control

Inertia, an inherent characteristic of synchronous generators, helps maintain grid stability by enabling a rapid response to such events ensuring that frequency stays within the specified range [2].

The power grid dynamics evolve with the ongoing shift toward renewable energy [3]. Unlike conventional counterparts, inverter-based sources do not contribute to grid inertia as they are not synchronously coupled to the grid [3], [4]. Thus, the overall grid inertia decreases since it is the combined effect of all online generation sources [5], as shown in (1).

$$M_{sys} = \sum_{i \in I} H_i * MVA_i \quad (1)$$

where I is the number of online synchronous machines, M_{sys} is the total kinetic energy stored in a grid, and H_i and MVA_i are any machine's inertia and base MVA.

With decreasing inertia, frequency response is more significantly impacted by an equivalent generation loss, as given by the swing equation below [6].

$$\Delta P = 2H \frac{df(t)}{dt} + Df(t) \quad (2)$$

where ΔP is the demand-supply power difference, H and $f(t)$ are grid inertia and frequency, respectively, and D is the load-damping factor. As shown in Fig. 1, for lower inertia, the nadir frequency deepens, the time to reach the nadir decreases, and the transient gap widens.

Where:

f_0 = pre-event nominal frequency,
f_s = final settling frequency, new steady-state value, where frequency stabilizes following contingency event,
f_n = the nadir frequency, the lowest frequency after the event,
d_{tr}= transient deviation = $f_s - f_n$,
d_{ss}= steady-state deviation = $f_0 - f_s$,
t_1 and t_2 are endpoints of the transient gap, a period where the system's frequency is below the f_s.

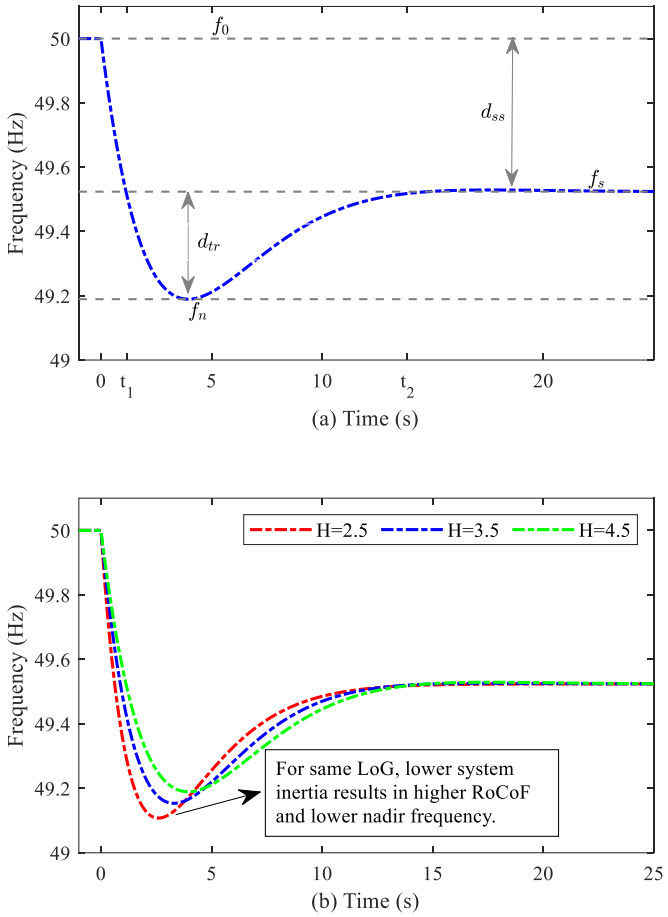

Fig. 1. (a) Details of system frequency response following a contingency event (b) Impact of inertia on system frequency response [7].

B. Aim and Objectives

This research aims to explore the concept of short-lived transient energy injection and assess its impact on power system stability. The key objectives of the study are:

- To analyze the low-order system frequency response (SFR) model to study the impact of reduced system inertia on frequency stability.
- To develop an alternative strategy for transient energy injection to compensate for the transient gap and validate this strategy through implementation in PowerFactory.
- To assess the impact of transient energy injection on its own and with conventional steady power injection and to identify the boundary value conditions when injected independently.
- To evaluate the limitations of transient energy injection and gauge its effectiveness and resilience during periods of volatile inertia and in situations with imprecise contingency size information.

II. Literature Review and Methodology

A. Literature Review

The shift towards renewables-rich power systems necessities faster external power injection as conventional primary frequency response (PFR) is not sufficiently fast [4], [8]. Fast frequency response (FFR) has been developed to fill this gap, acting within a second and thus being much faster than PFR [2], [9].

FFR, which combines inertial and primary frequency response, typically involves injecting active power generation or temporarily disconnecting the load to prevent frequency from reaching the under-frequency load shedding (UFLS) level [2], [4]. The effectiveness of an FFR scheme depends on response time, ramp-up rate, and resource capacity [9]. A short response time and large FFR resource capacity will only be effective if a high ramp-up rate is attainable [9].

FFR, through active power injection via batteries, can be safely activated at 100ms and supply the full output within 200ms [10], much faster than PFR, still slower than inertial response, which can get peak ramp-up power within 10ms of the event [10].

Therefore, when the initial RoCoF is very high, even the fastest control mechanism cannot arrest the frequency [2]. Thus, critical inertia represents the minimum inertia necessary in the power system to ensure the upper value of RoCoF. The critical inertia depends on the response time of the fastest injection resource, UFLS level, minimum load, maximum renewables penetration, and minimum synchronous sources online [8],[11]. Maintaining critical inertia is becoming challenging as more inverter-based generation is coming online. Alternatively, synchronous condensers and grid-forming inverters should be considered to provide the required inertia [12]. [13] suggests the interconnection as a better alternative in the long run and considers the importance of maintaining minimum inertia levels to help transition.

The inertia of a power system can vary significantly between regions, attributed to differences in renewable energy penetration patterns [14]. An FFR scheme that can address regional differences is crucial to prevent blackouts and system separation [9].

Determining the size of the loss of generation (LoG) using the initial RoCoF is also becoming challenging [15]. [16] estimates the center of inertia (CoI) RoCoF using local frequency measurements and presents an inflection point detector technique to remove the effect of local frequency oscillations. However, the increased penetration of renewables in power systems leads to a volatile inertia landscape [3]. A high RoCoF no longer signals a large LoG size. [15] proposes pinpointing the size and location of LoG events in a power system with abundant RES by introducing the method that leverages a superimposed circuit methodology, using available phasor measurement unit (PMU) measurements.

Existing fast-frequency response research mainly focuses on the response time, ramp-up rate, and injection capacity under the underlying conditions that the power injected is the same shape as the loss of generation, which is essentially a step or

more akin to a ramp response. However, a comprehensive analysis of power injection effectiveness and efficiency is lacking. Notably, no studies have been found to investigate the optimal shape of power injection for maximizing system stability or discussing short-lived transient energy injection, indicating a significant research gap that merits further investigation.

B. Research Approach and Methodology

The research begins with analysing stability challenges in modern power grids due to the increasing penetration of variable renewable energy sources. Using MATLAB simulations, a low-order SFR model, as explained in [7], is employed to study the impact of inertia, contingency size, and other system parameters.

The project progresses by developing a response to maximize stability by fixing the dropping frequency at the final steady-state level and determining the required injection to achieve that response. Subsequently, the research investigates the proposed injection's effectiveness, efficiency, and robustness.

The research has adopted a comprehensive methodology and workflow, as illustrated in Fig. 2.

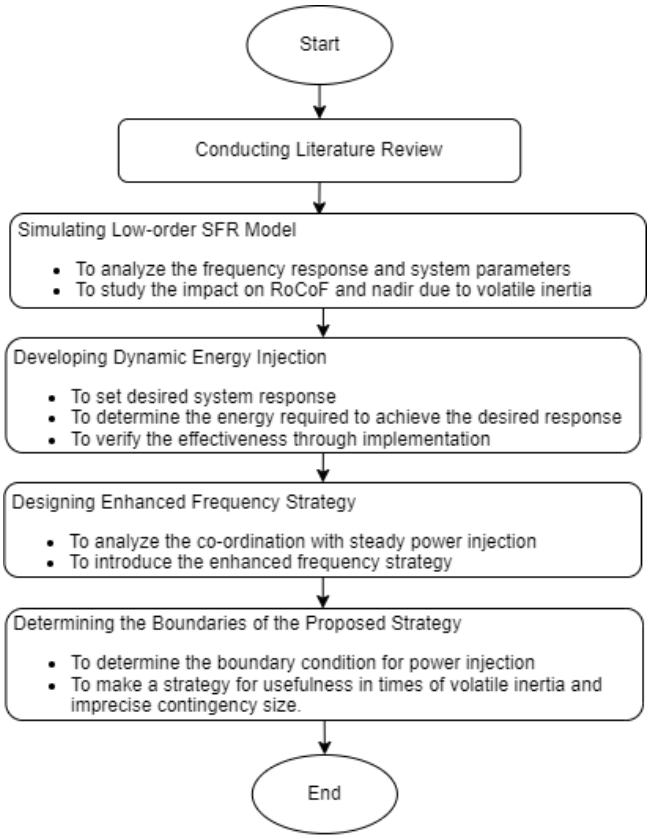

Fig. 2. Step-by-step research methodology.

III. Proposed Energy Injection and Implementation

A. Derivation of Proposed Energy Injection

The frequency response refers to the system's ability to stabilize frequency following sudden mismatch between generation and load [17]. It is an essential aspect of system reliability. Analysing the overall dynamics of power systems is challenging due to its inherent complexity. There are various mathematical models to simplify the frequency response for LoG events, including the low-order System Frequency Response (SFR) model, multi-machine SFR model, generic SFR model, and improved SFR model [7], [17], [18]. These models aim to gauge the system's behaviour following a contingency, allowing to make approximations and develop analytical solutions to frequency response without delving into the full complexity of the system [17].

This research utilizes the low-order SFR model for its simplicity and accuracy. The model is developed by only incorporating the largest time constant and generating unit inertia [7]. This model defines system behaviour with six fundamental parameters: governor droop (R), fraction of shaft power produced by high-pressure turbine (F_H), inertia (H), reheat time constant (T_R), Torque constant (K_m), and damping coefficient of load (D).

From these fundamental parameters, natural frequency (ω_n), damping frequency (ω_r), damping ratio (ζ) and other system parameters can be calculated as follows [7]:

$$\omega_n{}^2 = \frac{DR+K_m}{2HRT_R} \tag{3}$$

$$\zeta = \left(\frac{2HR+(DR+K_mF_H)T_R}{2(DR+K_m)}\right)\omega_n \tag{4}$$

$$\alpha = \sqrt{\frac{1-2T_R\zeta\omega_n+T_R{}^2\omega_n{}^2}{1-\zeta^2}} \tag{5}$$

$$\omega_r = \omega_n\sqrt{1-\zeta^2} \tag{6}$$

$$\varphi = \tan^{-1}\left(\frac{\omega_rT_R}{1-T_R\zeta\omega_n}\right) - \tan^{-1}\left(\frac{\sqrt{1-\zeta^2}}{-\zeta}\right) \tag{7}$$

As per this model, the frequency response in the Laplace domain, $\Delta F(s)$ for any power disturbance event can be given as follows [7]:

$$\Delta F(s) = G_{SFR}(s) \times P_d(s) \tag{8}$$

Where $P_d(s)$ is the power disturbance, and $G_{SFR}(s)$ is the SFR transfer function, solely dependent on fundamental system parameters and is given below [7]:

$$G_{SFR}(s) = \left(\frac{R\omega_n^2}{DR+K_m}\right)\left(\frac{1+T_Rs}{s^2+2\zeta\omega_ns+\omega_n^2}\right) \tag{9}$$

Equation (8) can be expressed in time domain as follows:

$$\Delta f(t) = g_{SFR}(t) * p(t) \tag{10}$$

where, "$*$" is the convolution operation.

Any contingency event is the step power disturbance and can be given as:

$$P_d(s) = \frac{P_{step}}{s} \tag{11}$$

And resulting frequency response can be given as follows [7]:

$$\Delta f(t) = \left(\frac{RP_{step}}{DR+K_m}\right)\left[1 + \alpha e^{-\zeta\omega_n t}\sin(\omega_r t + \varphi)\right] \tag{12}$$

The final steady-state frequency following an event can be determined by applying the final value theorem at (8) [7]:

$$\Delta f_s = \frac{RP_{step}}{DR+K_m} \tag{13}$$

And

$$f_s = f_0 + \Delta f_s \tag{14}$$

Similarly, when the frequency reaches its minimum point, its derivative becomes zero. From there, the time to reach the nadir is calculated [7]:

$$t_n = \frac{1}{\omega_r}\tan^{-1}\left(\frac{\omega_r T_R}{\zeta\omega_n T_R - 1}\right) \tag{15}$$

Substituting (15) in (12), Δf_n can be determined.

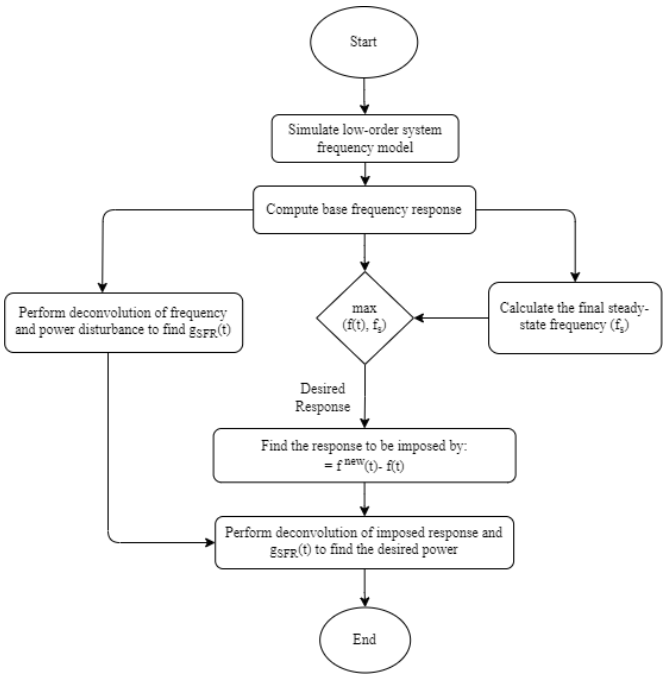

Fig. 3. Derivation of the proposed energy injection method.

The motivation for the optimal shape of injection comes from [19], where power deficit is derived following the contingency event. Due to the inertial response, this power deficit is more like a triangular shape than a step shape.

This study introduces a novel way to determine the transient energy injection. Instead of using a standard power injection, the proposed method emphasizes reaching the targeted output response and determining the power needed to attain that response.

Taking (9)-(11) from the low-order SFR model, the proposed transient injection is determined using the procedure shown in Fig. 3.

B. Performance Evaluation

This proposed energy injection is derived to target the transient gap and stabilize the system with only short-lived injection. The shape of this injection is fast ramp up followed by a relatively slow ramp down, though the proposed power does not have any standard geometrical shape, it does resemble with triangle.

$R = 0.10$ $\quad F_H = 0.3$ $\quad T_r = 8\,s$
$D = 0.1$ $\quad K_m = 0.95$ $\quad H = 4s$

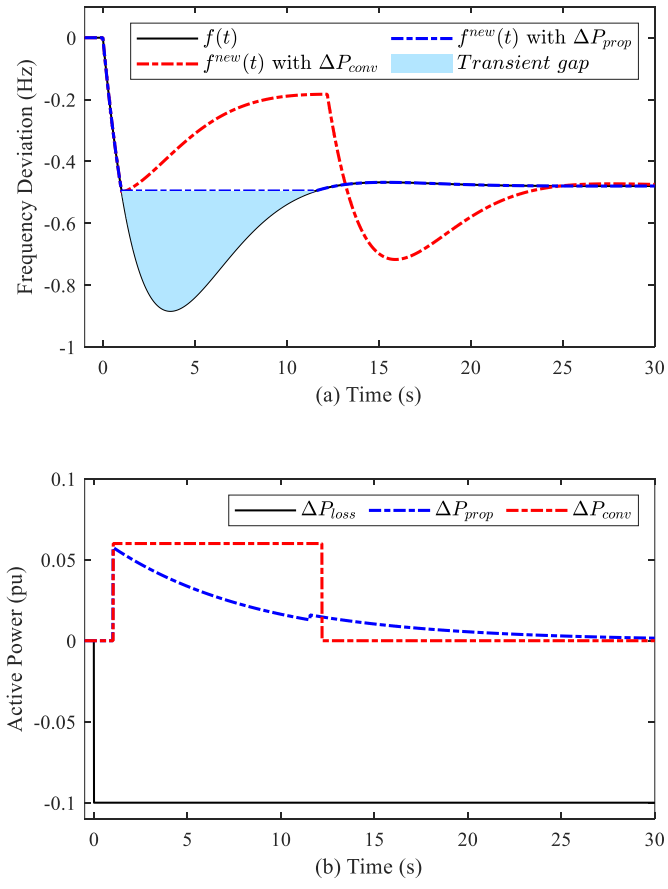

Fig. 4. (a) Fast-acting frequency containment with short-lived conventional and transient injection, (b) Conventional and proposed energy injection to achieve the containment for the same contingency size.

Fast acting frequency containment is generated with conventional and proposed power injection to compare. Fig. 4 illustrates the differences in fast frequency containment between the conventional and proposed approaches. With proposed injection, the system's overall stability is significantly improved by ensuring that the frequency remains at the settling value even if the secondary response is delayed.

For simplicity purposes, both injections are represented as having a step-like response. Specifically, the response is more akin to a ramp-up rather than an abrupt step. Whether the injection is gradual or near-to-step, the injection remains effective as long as the sources providing the peak power injection align with the proposed time of peak injection. This realization considers the fact that every source, including batteries, takes some time to ramp up [20], [21].

C. Most Energy Effective Injection

The proposed injection is based on using the least amount of energy to control frequency deviations and stabilize the system.

Frequency response following a contingency can be calculated as:

$$f(t) = g_{SFR}(t) * p_1(t) \tag{16}$$

where

$$f(t) = f(t) - f_0$$

After injecting the fast frequency response, new frequency can be given as:

$$\Delta f^{new}(t) = g_{SFR}(t) * p_2(t)$$

where

$$\Delta f^{new}(t) = f^{new}(t) - f_0$$

Given that:

$$\Delta f = f^{new}(t) - f(t)$$

Convolution follows linearity or has distributive property [22], therefore:

$$\Delta f(t) = g_{SFR}(t) * \big(p_2(t) - p_1(t)\big) \tag{17}$$

Now, referring to shaded area in Fig. 4, we determine transient gap as:

$$\int_0^\infty \Delta f\, dt = \int_0^\infty g_{SFR}(t) * \big(p_2(t) - p_1(t)\big)\, dt$$

Using convolution property, the integral over the convolution of two functions is the product of the integrals of the two functions [22], [23]:

$$\int_0^\infty \Delta f\, dt = \int_0^\infty \big(p_2(t) - p_1(t)\big)\, dt \int_0^\infty g_{SFR}(\tau) d\tau \tag{18}$$

Since

$$\int_0^\infty g_{SFR}(\tau)\, d\tau = G_{SFR}(0) = {}^{R}/_{DR + K_m} = constant$$

Thus,

$$\int_0^\infty \Delta f\, dt = constant \int_0^\infty \Delta p_{FFR}(t)\, dt \tag{19}$$

As, $f^{new}(t)$ coincides with $f(t)$ for all times other than interval $[t_1\ t_2]$. Thus, Δf is effectively zero for remaining period and thus, (18) can also be written as[23]:

$$\int_{t_1}^{t_2} \Delta f\, dt = constant \int_0^\infty \Delta p_{FFR}(t)\, dt \tag{20}$$

The goal is to minimize the gap in frequency response, making it the most energy efficient.

$$\int_0^\infty \Delta f\, dt = \int_0^\infty \big(f^{new}(t) - f(t)\big)$$

As $f(t)$ is unaffected by energy injection. Thus, $f^{new}(t)$ should be minimum under constraints of meeting required nadir frequency i.e., to the level of final steady state in this case.

D. Implementation in PowerFactory

The IEEE 39-bus model, representing the New England power system, is selected to implement the proposed strategy to verify its effectiveness [24]. The simulations are conducted on the default model available in the PowerFactory, except for making the load independent of frequency.

Center of inertia (CoI) frequency

There is no single point to measure the frequency of a power system, however, frequencies at different points oscillate around a curve, called as Center of inertia (CoI). To calculate the CoI frequency, the local speeds of all online generators can be weighted average [5].

$$f_{CoI} = \sum_{i=1}^{N} \frac{H_i S_i f_i}{H_i S_i} \tag{21}$$

Where f_{CoI} is the CoI frequency and H_i, S_i and f_i are respectively the inertia, MVA capacity and equivalent electrical frequency of any generator. Thus, (2) can also be given as:

$$2H_{CoI} \frac{df_{CoI}(t)}{dt} + D\Delta f_{CoI}(t) = \Delta P(t) \tag{22}$$

CoI frequency serves as a pivotal metric in power system analysis.

Model Specification and Proposed Injection Strategy

The 39-bus model contains ten generators and has an overall inertia of 4.582s. It has 6140MW demand on the default case, and the loss of generator 3, which contributes around 650MW, makes around 10% of the total load thus, it is equivalent to LoG of -0.1058 pu. Frequency response is calculated for loss of

generator-3 and power injection was determined using the methodology described in Fig. 3.

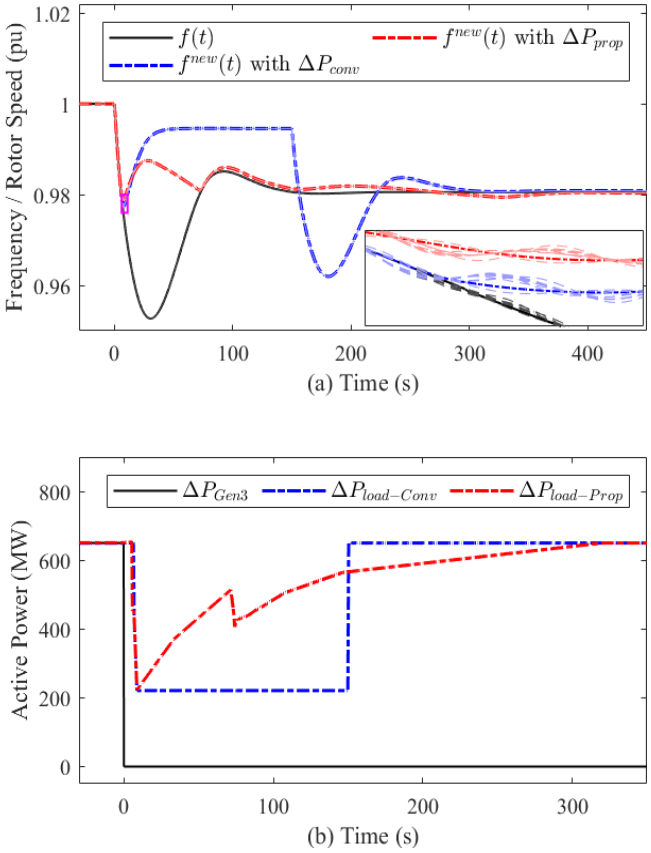

Fig. 5 (a) Fast-acting frequency containment in PowerFactory with a zoomed-in section highlighting the local speeds of the generators., (b) Load manipulation devised to achieve frequency containment, only specific portion of the load has been manipulated to formulate the strategy.

The proposed injection was approximated to the nearest combination of triangular shapes for loss of generator 3, and results are compared with short-time conventional response. As shown in Fig. 5, both FFRs are set up by reducing the load rather than injecting the power. Given the brief time duration, manipulating load could be an effective strategy, capitalizing on the flexibility provided by smart loads [4], [25].

Since the shape of proposed power is not regular and injected power is only its good approximation and thus, does not completely flatten the frequency response curve as desired, however, it stabilizes the frequency and gives good essence of the effectiveness of the transient injection.

IV. Orchestrating Frequency Regulation: A Triad of Transient, Steady, and Enhanced Injections

A. Impact of Transient Energy Injection

Transient energy injection aims to fill the transient gap and improve the nadir frequency. Any change in frequency following a demand-supply mismatch can be given as:

$$\int_0^\infty \Delta f \, dt = \int_0^\infty g_{SFR}(t) * \Delta p(t) \, dt$$

The power required to flatten the frequency containment curve can be found using (20):

$$\int_{t_1}^{t_2} (f_s - f(t)) \, dt = \int_0^\infty g_{SFR}(t) * \Delta p_{FFR}(t) \, dt \tag{23}$$

Let β represent the percentage compensation for the transient gap. At $\beta = 1$, nadir frequency approximates the settling frequency. Thus, it involves transient energy to arrest decreasing frequency, driving the containment to the steady-state level. The relationship between the energy needed to raise the nadir to the steady state, E, and the energy for any new nadir, E' can be described as:

$$E' = \beta \, E \tag{24}$$

As convolution follows the homogeneity property [22], thus:

$$\int_0^\infty g_{SFR}(t) * (\beta \, \Delta p_{FFR}(t)) \, dt = \beta \int_{t_1}^{t_2} (f_s - f(t)) \, dt$$

Therefore, the new frequency corresponding to changing transient energy injection can be given as:

$$f^{new}(t) = \begin{cases} f(t) & t < t_1 \text{ and } t_2 < t \\ f(t) + \beta\big(f_s - f(t)\big) & t_1 \le t \le t_2 \end{cases} \tag{25}$$

Equation (25) covers the compensation effect on the nadir. Time to reach the nadir remains the same for $\beta < 1$ as given in (15) and reduces to t_1 as β approaches 1 as shown in Fig. 6.

$$t_n{}^{new} = \begin{cases} t_n & \beta < 1 \\ t_1 & \beta \ge 1 \end{cases} \tag{26}$$

Moreover, the compensation level required to arrest the frequency prior to the threshold nadir can be given as follows:

$$\beta = \frac{f_n{}^{new} - f_n}{f_s - f_n} \tag{27}$$

Here the shape of the injection, starting time, and duration remain essentially the same. The frequency curve is not fully flattened for $\beta < 1$. However, it effectively controls the RoCoF and arrests the nadir. Alternatively, for every desired nadir, new transient energy injection needs to be calculated to fully flatten the curve.

Compensated frequency linearly varies with the transient energy injection if the overall inertia of the system is not significantly impacted by the sources injecting the fast-frequency energy. However, energy beyond $\beta = 1$ cannot further improve the nadir frequency.

$R = 0.10$ $F_H = 0.3$ $T_r = 8\ s$
$D = 0.1$ $K_m = 0.95$ $H = 4s$

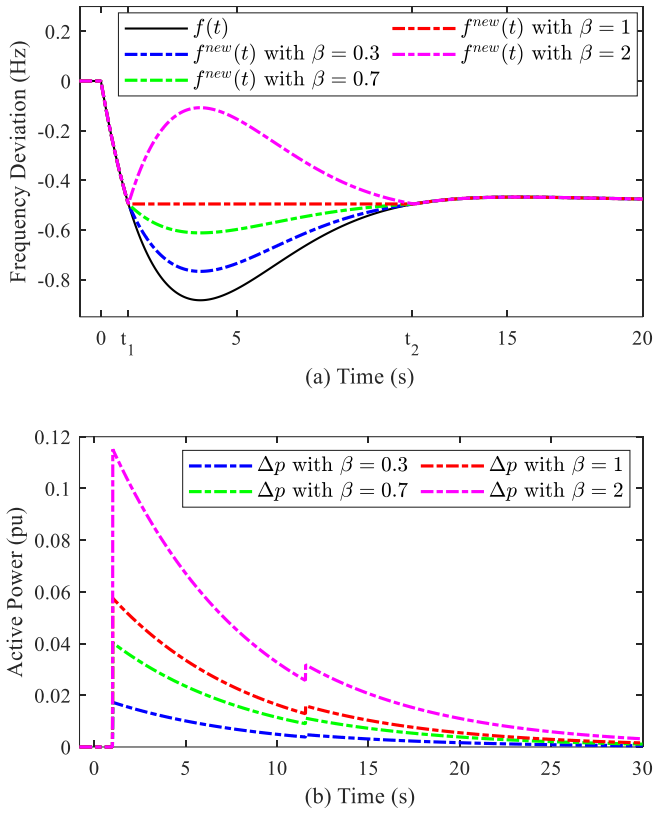

Fig. 6. (a) Fast-acting frequency containment with varying transient injection, (b) energy injection required to achieve the containment.

B. Effects and Limits of Transient Energy Overcompensation in Power Systems: A Sensitivity Analysis

Post-contingency power systems can endure transient energy overestimation to a considerable extent without causing frequency overshoots, thanks to its short-lived nature.

If $\beta > 1$, the transient gap is overcompensated, the nadir equals the final steady-state value, and additional energy results in part of the frequency containment being higher than f_s.

Overcompensation is when power drives the max frequency above the final steady-state, f_s and overshoot refers to any frequency exceeding the pre-event steady-state, f_0. The maximum overcompensation limit (MOL) determines the permissible overcompensation limit without causing any overshoot.

$$MOL = \left|\frac{f_0 - f_s}{f_s - f_n}\right| \tag{28}$$

For SFR parameters given in Fig. 6, steady-state and nadir frequency are:

$\Delta f_s = -0.473$ Hz and $\Delta f_n = -0.8832$Hz.

Using (28), allowed overcompensation limit ≈ 115%. Thus, even double the proposed energy injection does not cause any frequency overshoot, shown in Fig. 6.

Like (25), overshoot frequency can be given as:

$$f_{overshoot} = f_n + \beta(f_s - f_n) \tag{29}$$

This adaptability ensures that the injection remains effective in times of volatile inertia, discussed further in Section-V.

Impact of System Inertia

Equation (27) shows that MOL depends on the nadir and final steady-state frequencies. Allowed compensation depends upon the nadir frequency, which depends on the system's inertia, as shown in Fig. 1. A decrease in system inertia results in lower nadir and, consequently, a reduced MOL, shown in Table I.

$R = 0.10$ $F_H = 0.3$ $T_r = 8\ s$
$D = 0.1$ $K_m = 0.95$

TABLE I
CHANGE IN OVERCOMPENSATION LIMITS WITH INERTIA

Inertia (s)	MOL (%)
6	162.9418
5	149.3096
4	135.5401
3	121.5822
2	99.9967

Though MOL is reduced in the low-inertia power system, there is substantial capability for tolerating the transient energy overcompensation.

Impact of Size of Contingency

As shown in (12), the change in frequency is linearly proportional to the contingency size. Both steady-state frequency, f_s and nadir frequency, f_n are directly proportional to the size of LoG. Therefore, there is no impact of size of LoG on the MOL. Limits for overcompensation are solely dependent on the system parameters.

C. Steady-State Power Injection: Effects and Coordination

Transient energy injection targets explicitly to improve the nadir frequency, and the final settling frequency remains the same as without any compensation.

We define λ is the fractional compensation for the steady-state response. This compensation aims to restore the system to its pre-fault frequency level. This compensation is like the secondary frequency response that may take sufficient time to ramp up as the prime concern of faster RoCoF and deep nadir is tackled with the transient energy injection. The only

difference between this and the secondary response is that short-lived energy does not improve the final steady-state response, unlike the typical primary frequency response. To bring the system to its nominal value, steady-state power injection must equal to the power loss.

With transient energy injection and steady power, frequency containment would depend on the start time and ramp-up rate of steady power. However, if steady power starts once frequency stabilizes at f_s then nadir, and final steady frequency can be given as:

$$f_n{}^{new} = f_n + \beta(f_s - f_n) \tag{30}$$

$$f_s{}^{new} = f_s + \lambda(f_0 - f_s) \tag{31}$$

While the transient energy injection does not need to completely die out before the activation of steady power, however, coordination between them is crucial to avoid potential overshoot.

$R = 0.10$ $F_H = 0.3$ $T_r = 8\ s$
$D = 0.1$ $K_m = 0.95$ $H = 4s$

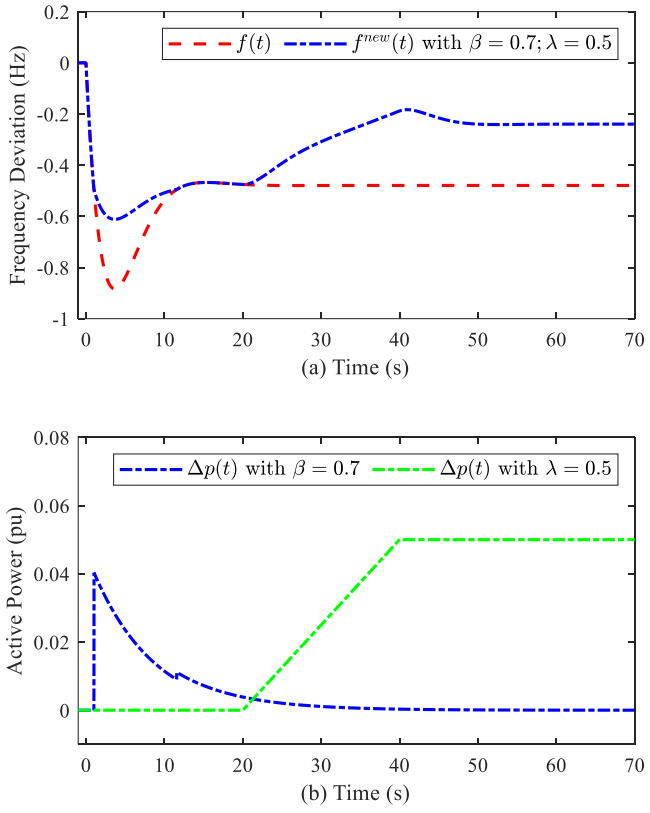

Fig. 7. A well-coordinated comprehensive response with transient energy correcting the required nadir and steady power correcting steady state error.

D. Enhanced Power Injection: Impact and Limitations

Coordinating transient energy injection with steady power yields specific outcomes, with roles bifurcated between β for transient error, d_{tr} reduction and λ for addressing steady-state errors, d_{ss}. The transient energy injection (flattening the curve) can complement steady-state injection to improve the nadir further, above the transient gap.

We introduce the concept of enhanced injection γ, which represents the improvement of nadir beyond the range of energy transient injection, β and the removal of the steady-state error. It symbolizes the transient and steady injection combination, causing the frequency containment curve to flatten above the f_s.

$R = 0.10$ $F_H = 0.3$ $T_r = 8\ s$
$D = 0.1$ $K_m = 0.95$ $H = 4s$

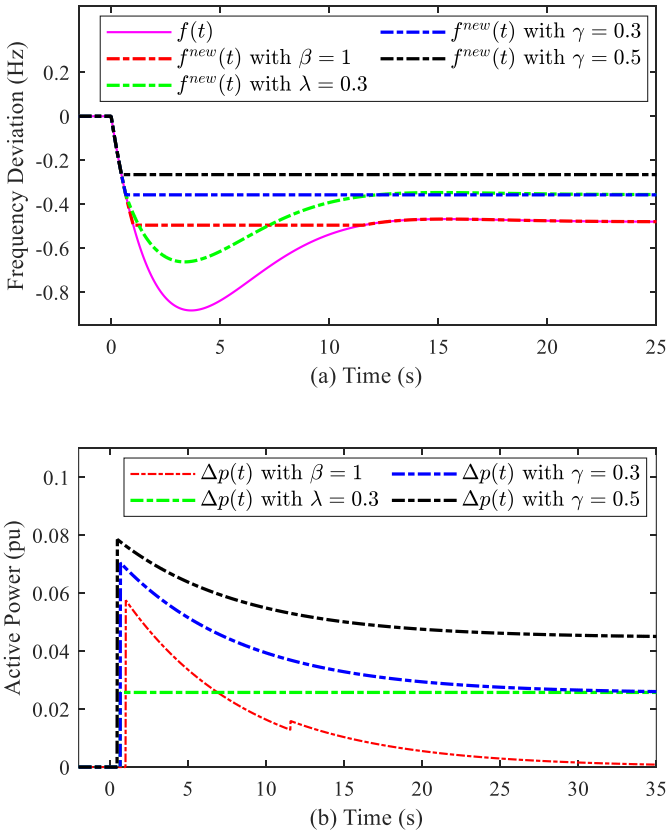

Fig. 8. (a) Fast-acting frequency containment with varying enhanced power injection, (b) enhanced power injection required to achieve the containment.

Frequency containment with the enhanced power injection can be given as follows:

$$f^{new}(t) = \begin{cases} f(t) & t < t_1 \\ f_s + \gamma d_{ss} & t \geq t_1 \end{cases} \tag{32}$$

where t_1 is the time when curve starts to flatten.

As illustrated in Fig. 8, the blue and green curves, starting simultaneously, represent different power injection approaches. While both aim for the same steady-state level, the blue curve benefits from additional transient energy, leading to smoother frequency containment and a significantly improved nadir

frequency.

The enhanced injection coefficient γ represents a hybrid control strategy, combining transient and steady elements. As the value of γ increases from 0 to 1, the steady part increases, and the transient part decreases. Unlike β and λ, γ does not serve as a multiplicative factor of power. Instead, it is the scaling factor of nadir improvement from the naturally settling frequency to the pre-event level. When $\gamma = 0$, it does not imply the absence of energy injection. Rather, it depicts a transient energy injection with $\beta = 1$, thereby bringing the nadir to the settling frequency, f_s.

If all measurement data and steady power equal to the loss of generation are available right after the contingency, with appropriate ramp-up time then it can serve sufficiently and eliminates the need of the transient energy injection, which represents the $\gamma \approx 1$. The limitation of the upper value of γ depends not only on the amount of capacity available to inject but also on the RoCoF following an event as some minimum time is required to analyse contingency event and ramp up the service [8]. Thus $\gamma \approx 1$ is not achievable.

V. Managing Volatile Inertia in Power System: Estimation, Energy Injection, and Contingency Planning

Unlike conventional injection, which solely depends upon the size of the contingency, proposed transient compensation also depends on system parameters. Inertia is one such critical factor that is volatile in modern systems. It does not impact the settling frequency, instead only on the initial RoCoF, i.e., reflected in the nadir frequency and time to reach the nadir. This section deals with challenges associated with the volatility of inertia and proposes a way out.

A. Estimating the System Inertia

The system inertia can be estimated by assuming all other low-order SFR parameters and the contingency size are known. The proposed approach utilizes an error function quantifying the deviation between the modelled and actual frequency over time. Using (3)–(8), a function of frequency can be formulated in terms of inertia and time and compared with the known CoI frequency.

The value of inertia that minimizes the error function is obtained through the optimization process:

$$H_{est} = arg\,min_H\, J(H) \tag{33}$$

where

$$J(H) = \sum\left(f_{measured}(t) - f_{calculated}(t, H)\right)^2$$

Once the measured CoI frequency is available, it requires only calculation time to find the system inertia. This approach is, however, prone to the inaccuracies of data of other SFR parameters and the measured frequency.

A comprehensive sensitivity analysis was conducted to examine the potential inaccuracies in the system model parameters that could impact inertia estimation. It was determined that the measured frequency, the size of the contingency, ΔP_{loss} and the torque constant, K_m are particularly crucial among the parameters.

Despite these limitations, this method provides a valuable starting point for system inertia estimation, narrowing down the range of potential inertia values and enhancing the effectiveness of system operation and planning.

B. Impact of Volatile Inertia on Proposed Compensation

Key characteristics of proposed transient energy injection are the peak of injection, slope– thus the duration of injection, start time, and overall energy injected.

SFR fundamental parameters and contingency size are known, then the behaviour of required energy injection with changing inertia can be determined as shown in Fig. 9.

The required energy injection is proportional to the size of the transient gap, as determined in (20), and the size of the transient gap changes with the inertia, as shown in Fig. 1. Lower inertia results in a wider transient gap, and vice versa. Therefore, for low inertia, higher energy is required. It also requires the injection to start early due to higher RoCoF, illustrated in Fig. 9. Since this injection can tolerate the overcompensation. Thus, if the system has very volatile inertia, the injection should be done considering the lowest inertia so that sufficient energy can be injected.

$R = 0.10$ $\quad F_H = 0.3$ $\quad T_r = 8\ s$
$D = 0.1$ $\quad K_m = 0.95$ $\quad P_{loss} = -0.1\ pu$

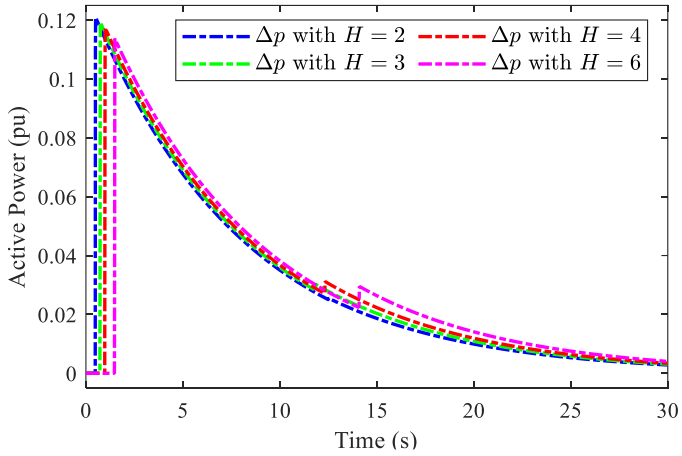

Fig. 9. Transient energy injection required to fully flatten the frequency containment curve for known contingency size and different inertia values.

C. Resilience Against Errors

Uncertainty in the System Inertia

There might be inaccuracies in estimating inertia, and the proposed injection varies with the inertia. Despite the variations in inertia and the associated start time and size of transient injection, the system is stabilized when power is injected under assumptions of a lower inertia value, as illustrated in Fig. 10.

$R = 0.10$ $F_H = 0.3$ $T_r = 8\ s$
$D = 0.1$ $K_m = 0.95$ $P_{loss} = -0.1\ pu$

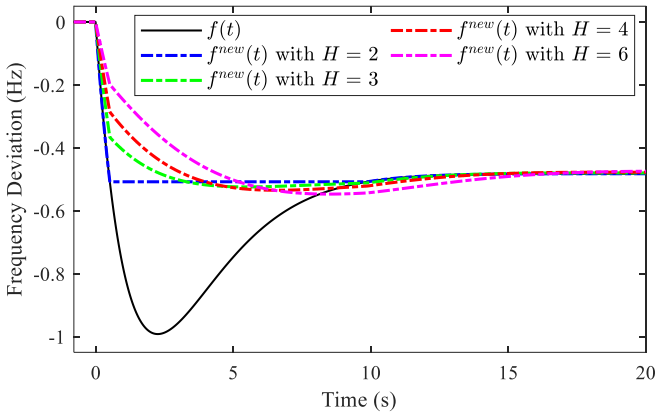

Fig. 10. Frequency containment for different system inertia with constant transient energy calculated for H=2s to realize the impact of volatile inertia.

This finding suggests that in situations where the exact inertia is unknown, system operators can employ a conservative estimate without compromising system stability. Moreover, regarding the possible error in inertia that is subject to inaccuracies in the data of remaining SFR parameters, tolerance for all parameters should be taken such that it may result in lower inertia than actual rather than higher inertia.

Uncertainty in the Size of Contingency due to Volatile Inertia

This section builds on the insight that LoG size is unknown, however, the centre of inertia frequency can still be obtained from local frequencies, as detailed in [16]. Differentiating the (12), the following can be obtained.

$$\frac{df(t)}{dt} = \left(\frac{\omega_n \alpha R P_{step}}{DR + K_m}\right) e^{-\varsigma \omega_n t} \sin(\omega_r t + \varphi_1) \tag{33}$$

Using (33) or the swing equation, it can be deduced that the RoCoF following a LoG is proportional to the size of the contingency. If inertia is known, using the swing equation, measuring RoCoF can determine the actual contingency size, and energy injection can be proposed accordingly.

Due to continuous changes in the energy mix and renewables' penetration, precise inertia value might not be known [3]. However, depending on the possible generation scenarios in a power grid, a range can be determined in which inertia lies with 100% confidence. Based on this, frequency response has been predicted using the boundary values of inertia and initial CoI frequency.

At measured RoCoF, if the contingency is estimated with the highest value in inertia, then the base frequency response will have the lowest nadir and the widest transient gap, as shown in Fig. 11. This can be chosen to predict the transient energy injection due to the tolerance of transient energy overcompensation.

$R = 0.10$ $F_H = 0.3$ $T_r = 8\ s$
$D = 0.1$ $K_m = 0.95$ $H = [3\ 4]$

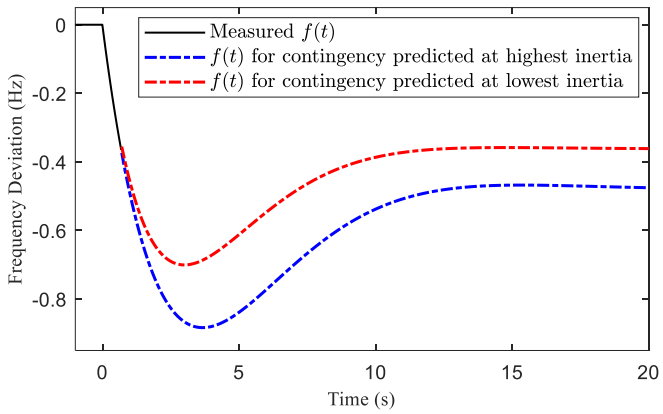

Fig. 11. Frequency response based on different values of inertia-estimated contingency sizes.

If $H \in [H_{min}\ H_{max}]$ then error in estimation can be given as:

$$e = \left|\frac{H_{predicted} - H_{actual}}{H_{max} - H_{min}}\right| \tag{34}$$

The highest value from a specified inertia range is chosen to estimate the contingency size. The consequences are analyzed when the actual inertia is at the lowest end of the specified range, or there is maximum error in estimation.

Due to tolerance for over-injection of transient energy, as shown in Fig. 12(a), the green curve shows that the system remains stable, and the nadir is contained even when estimated inertia has the maximum error.

If inertia is known in a specific range and CoI frequency can be estimated using local frequencies, then the transient energy injection can be proposed without knowing the contingency size. Under this approach, contingency size should be estimated at the highest value of inertia in the range while starting time for energy injection and proposed injection should be determined based on the minimum inertia. This strategically crafted method aims to fortify system stability in the face of inertia's inherent volatility and the uncertainty that often accompanies the determination of contingency size.

$R = 0.10$ $F_H = 0.3$ $T_r = 8\ s$
$D = 0.1$ $K_m = 0.95$ $H = [3\ 4]$

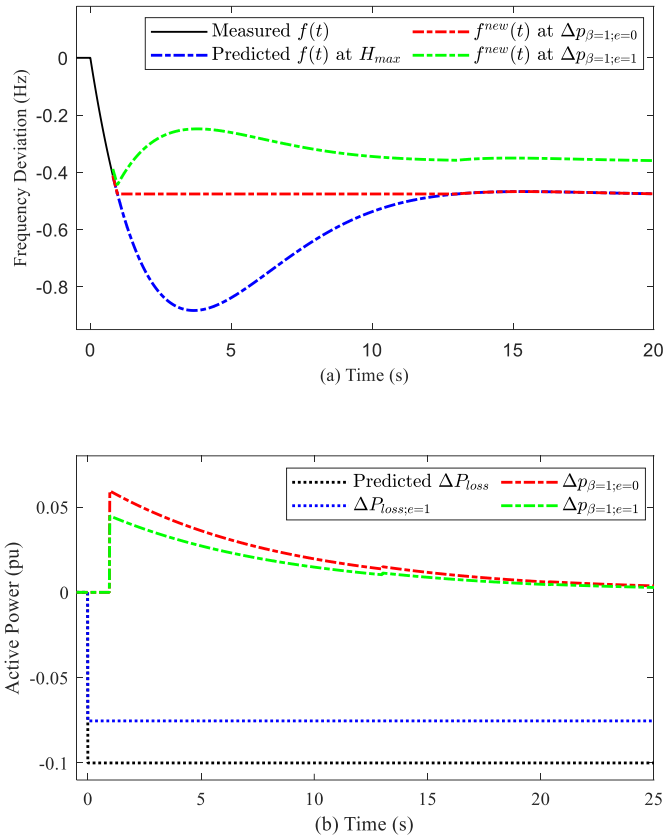

Fig. 12. (a) Fast-acting frequency containment with transient energy injection for inertia based contingency size estimation, (b) Transient energy injection for inertia based contingency size estimation.

VI. Conclusion

A. Project Aims and Objectives

The project meets its outlined aim and objectives and successfully puts forth the concept of transient energy injection and its implications in the control strategies for contingency events. However, some noteworthy observations merit attention.

While the proposed transient energy injection improves the nadir frequency but does not flatten the curve for $\beta < 1$ as a constant power shape has been utilized. Comparing the proposed injection with the most optimized version could provide further insights into the efficacy and robustness of short-lived injections.

The utilized low-order SFR model is reasonably accurate and straightforward. The obtained results are verified through implementation in PowerFactory. However, more sophisticated models are available, especially for low inertia power systems, and can help derive the analytical solution in terms of fundamental system parameters.

While the default IEEE-39 bus model was sufficient for this study, it has very high inertia. It could be addressed by replacing a few generators with RES. A closer alignment between the SFR model parameters and the model used in PowerFactory would also have enhanced the coherence.

The DPL feature was unavailable in the available license of PowerFactory, so the time series of the proposed injection could not be loaded. Thus, approximated triangular shape was injected, and the frequency containment curve was not exactly flattened.

Addressing these points could further enhance the impact of this work.

B. Significant Technical Achievement

This paper introduces a novel short-lived transient energy injection approach to address the transient gap and enhance frequency stability in power systems. It also examines the boundary field conditions and comprehensively lays out the challenges and advantages of the proposed energy injection.

C. Future Work

The proposed power injection strategy described in this research provides an energy-efficient and robust complement to conventional techniques. One key challenge is the necessity for precise timing for this injection. Unlike conventional injection, where faster is preferable, this method requires exact coordination. An injection that is too early may also not perform well. Implementing a closed-loop control system could be a potential avenue to overcome this limitation, but it was outside the scope of the current research. This work provides the behaviour of the proposed injection; however, an analytical expression has yet to be derived, and sources that can provide the proposed transient injection need to be identified.

While the research sets a promising direction, it recognizes that there is room for further exploration. The study serves as an initial step toward new solutions and emphasizes the need for continuous efforts to optimize the shape of FFR injections and enhance overall system stability.

D. Reflection

This project gave me a comprehensive understanding of frequency stability, the associated challenges, and the contemporary solutions shaping the field. The in-depth exploration of these complex topics enhanced my knowledge of engineering mathematics. I also learned much about practical applications, such as working with PowerFactory.

Engaging in all aspects of research, including report writing, was a rewarding. While writing this report, I realized the importance of presenting technical information clearly and concisely, ensuring it is accessible to a broader audience.

Overall, the project was a rich learning experience that deepened my technical knowledge and fostered personal and professional growth.

APPENDIX

Impact of Inertia on Transient Gap

In Fig. 13, frequency response is calculated at H=2 and 4.5s, and the non-overlapping gap is compared. Decreasing inertia increases the RoCoF, thus, decreasing the nadir frequency and decreasing the time to reach the nadir and settling frequency, and both counteract each other. However, the overall effect is that the transient gap increases with low inertia.

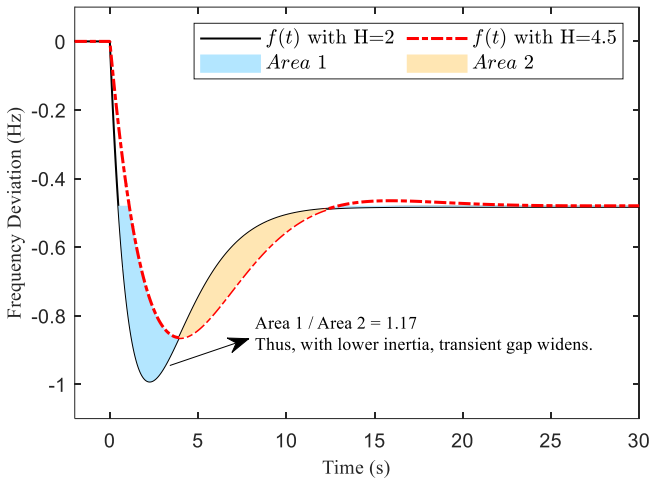

Fig. 13. Impact of inertia on the area of the transient gap.

ACKNOWLEDGMENT

This work is dedicated to the unwavering love of my mother, Sheela, and in memory of my late father, Partab Rai. My profound gratitude goes to the constant source of inspiration, my elder brother, Love Kumar. I am deeply grateful to the Commonwealth Scholarship Commission for funding my master's studies. A special note of thanks is reserved for my supervisor, Dr. Sadegh Azizi. Our enriching conversations have significantly shaped this research and broadened my understanding of the subject. Lastly, my heartfelt thanks extend to friends, peers, and all who have contributed to this fulfilling experience.

REFERENCES

[1] "Connection Conditions," National Grid ESO, Jan. 2023. Accessed: Apr. 23, 2023. [Online]. Available: https://www.nationalgrideso.com/document/33846/download

[2] "Fast Frequency Response Concepts and Bulk Power System Reliability Needs," NERC, Mar. 2020. Accessed: Apr. 20, 2023. [Online]. Available: https://www.nerc.com/comm/PC/InverterBased%20Resource%20Performance%20Task%20Force%20IRPT/Fast_Frequency_Response_Concepts_and_BPS_Reliability_Needs_White_Paper.pdf

[3] P. Tielens and D. Van Hertem, "The relevance of inertia in power systems," *Renew. Sustain. Energy Rev.*, vol. 55, pp. 999–1009, Mar. 2016, doi: 10.1016/j.rser.2015.11.016.

[4] P. Denholm, T. Mai, R. Kenyon, B. Kroposki, and M. O'Malley, "Inertia and the Power Grid: A Guide Without the Spin," NREL/TP-6A20-73856, 1659820, MainId:6231, May 2020. doi: 10.2172/1659820.

[5] A. Ulbig, T. S. Borsche, and G. Andersson, "Impact of Low Rotational Inertia on Power System Stability and Operation," *IFAC Proc. Vol.*, vol. 47, no. 3, pp. 7290–7297, Jan. 2014, doi: 10.3182/20140824-6-ZA-1003.02615.

[6] P. Kundur, *Power System Stability and Control*, Second Edition. New York: McGraw Hill LLC, 2022.

[7] P. M. Anderson and M. Mirheydar, "A low-order system frequency response model," *IEEE Trans. Power Syst.*, vol. 5, no. 3, pp. 720–729, Aug. 1990, doi: 10.1109/59.65898.

[8] "Inertia: Basic Concepts and Impacts on ERCOT Grid," ERCOT, 2018. Accessed: Apr. 20, 2023. [Online]. Available: https://www.ercot.com/files/docs/2018/04/04/Inertia_Basic_Concepts_Impacts_On_ERCOT_v0.pdf

[9] Q. Hong *et al.*, "Fast frequency response for effective frequency control in power systems with low inertia," *J. Eng.*, vol. 2019, no. 16, pp. 1696–1702, Mar. 2019, doi: 10.1049/joe.2018.8599.

[10] "Batteries_Beyond_the_Spin.pdf." Accessed: Apr. 22, 2023. [Online]. Available:http://everoze.com/app/uploads/2019/11/Batteries_Beyond_the_Spin.pdf

[11] "Operability Strategy Report 2023." Accessed: Apr. 22, 2023. [Online]. Available: https://www.nationalgrideso.com/document/273801/download

[12] L. Pagnier and P. Jacquod, "Optimal Placement of Inertia and Primary Control: A Matrix Perturbation Theory Approach," *IEEE Access*, vol. 7, pp. 145889–145900, 2019, doi: 10.1109/ACCESS.2019.2945475.

[13] L. Mehigan, D. Al Kez, S. Collins, A. Foley, B. Ó'Gallachóir, and P. Deane, "Renewables in the European power system and the impact on system rotational inertia," *Energy*, vol. 203, p. 117776, Jul. 2020, doi: 10.1016/j.energy.2020.117776.

[14] P. Ashton, C. Saunders, G. Taylor, A. Carter, and M. Bradley, "Inertia Estimation of the GB Power System Using Synchrophasor Measurements," *Power Syst. IEEE Trans. On*, vol. 30, pp. 701–709, Mar. 2015, doi: 10.1109/TPWRS.2014.2333776.

[15] J. Sánchez Cortés, M. Rezaei Jegarluei, P. Aristidou, K. Li, and S. Azizi, "Size/location estimation for loss of generation events in power systems with high penetration of renewables," *Electr. Power Syst. Res.*, vol. 219, p. 109242, Jun. 2023, doi: 10.1016/j.epsr.2023.109242.

[16] M. Sun, G. Liu, M. Popov, V. Terzija, and S. Azizi, "Underfrequency Load Shedding Using Locally Estimated RoCoF of the Center of Inertia," *IEEE Trans. Power Syst.*, vol. 36, no. 5, pp. 4212–4222, Sep. 2021, doi: 10.1109/TPWRS.2021.3061914.

[17] H. Huang *et al.*, "Generic System Frequency Response Model for Power Grids With Different Generations," *IEEE Access*, vol. 8, pp. 14314–14321, 2020, doi: 10.1109/ACCESS.2020.2965591.

[18] Q. Shi, F. Li, and H. Cui, "Analytical Method to Aggregate Multi-Machine SFR Model With Applications in Power System Dynamic Studies," *IEEE Trans. Power Syst.*, vol. 33, no. 6, pp. 6355–6367, Nov. 2018, doi: 10.1109/TPWRS.2018.2824823.

[19] S. Azizi, M. Sun, G. Liu, and V. Terzija, "Local Frequency-Based Estimation of the Rate of Change of Frequency of the Center of Inertia," *IEEE Trans. Power Syst.*, vol. 35, no. 6, pp. 4948–4951, Nov. 2020, doi: 10.1109/TPWRS.2020.3014818.

[20] N. W. Miller, M. Shao, R. D'aquila, S. Pajic, and K. Clark, "Frequency Response of the US Eastern Interconnection Under Conditions of High Wind and Solar Generation," in *2015 Seventh Annual IEEE Green Technologies Conference*, Apr. 2015, pp. 21–28. doi: 10.1109/GREENTECH.2015.31.

[21] X. Yuan, J. Hu, and S. Cheng, "Multi-time scale dynamics in power electronics-dominated power systems," *Front. Mech. Eng.*, vol. 12, no. 3, pp. 303–311, Sep. 2017, doi: 10.1007/s11465-017-0428-z.

[22] P. D. Heeger, "Signals, Linear Systems, and Convolution", [Online]. Available: https://www.cns.nyu.edu/~david/handouts/convolution.pdf

[23] J. Sánchez Cortés, M. Rezaei Jegarluei, and S. Azizi, "Optimal Frequency Containment in Power Systems: The Future is Now with a New Paradigm." in International Conference on Energy Technologies for Future Grids (IEEE ETFG23) (Accepted).

[24] "39 Bus New England System." in Software Documentation - PowerFactory. DIgSILENT, Gomaringen, Germany.

[25] V. Trovato, I. M. Sanz, B. Chaudhuri, and G. Strbac, "Advanced Control of Thermostatic Loads for Rapid Frequency Response in Great Britain," *IEEE Trans. Power Syst.*, vol. 32, no. 3, pp. 2106–2117, May 2017, doi: 10.1109/TPWRS.2016.2604044.